31st International Conference Nuclear Energy for New Europe
NENE 2022 September 12-15 PORTOROŽ SLOVENIA

Modelling Gamma Calorimetry Experiment with JSIR2S Code

Klemen, Ambrožič[a], Vladimir Radulović[a], Hubert Carcreff [b], Damien Fourmentel [c], Luka Snoj [a]

[a] Reactor Physics division F8
Jožef Stefan Institute
Jamova cesta 39
1000, Ljubljana, Slovenia

[b] CEA, Service d'études des réacteurs et de mathématiques appliquées
Université Paris-Saclay,
3 rue Joliot Curie
Gif sur Yvette 91191, France

[c] DES, IRESNE, DER, SPESI
CEA Cadarache
St Paul Lez Durance 13108, France

klemen.ambrozic@ijs.si, vladimir.radulovic@ijs.si, hubert.carcreff@cea.fr, damien.fourmentel@cea.fr, luka.snoj@ijs.si

ABSTRACT

In this paper we present the preliminary results of reproducing the experimental determination of nuclear heating in fission and fusion relevant materials by simulations. The experiments were performed inside the Central irradiation channel of the Jožef Stefan Institute (JSI) TRIGA mk. II reactor at reactor power levels of 100 kW and 250 kW respectively.
The modelling includes both the simulations of the prompt radiation field by the MCNP code and the gamma radiation field due to decay of radioactive isotopes, produced during reactor operation. Individual contributions both in term of particle types (neutrons vs. gamma rays vs. electrons) and in terms of generation time (prompt vs. delayed) will be evaluated and compared to the measured values.

1 INTRODUCTION

An extensive nuclear heating measurement campaign was performed in 2021 at the JSI TRIGA reactor, with material samples made of low activation steel Eurofer97, aluminium 6063, graphite R6650 and 99.95 % pure tungsten. The calorimeter design was based on previous versions of CEA developed CALMOS [1] and CARMEN [2] differential calorimeters for the OSIRIS reactor, and modified for lower heating levels of the JSI TRIGA reactor [3]. A separate calorimeter without a sample was used to evaluate the heating levels to the sample by measuring the temperature difference between the calorimeter with and without the sample, and by injecting the power to an electrical heater of the empty calorimeter, until the temperature profile matches the profile of the calorimeter with sample (also called zero method). While the measurements were generally successful and within the predicted heating levels, some unexpected

non-linear effects were observed, leading to a lower level of confidence in the obtained results. While preliminary simulations on expected levels of nuclear heating were performed in order to aid with the calorimeter design [4] , it was decided to simulate the entire experimental campaign to observe both the quality of experimental data and the applicability of the JSIR2S code [5] to nuclear heating problems.

2 MODELLING CONSIDERATIONS

The simulations were performed with a modified version of Monte Carlo particle transport code MCNP v.6.1 [6], the JSIR2S code [5] and ENDF/B VIII.0 nuclear data libraries [7]. Isotopic composition of modelled materials was obtained using MATSSF code [8]. The reactor's model geometry was based on the reference model [9] with the core configuration reflecting the core configuration during irradiation and new triangular channels [10, 11], displayed in Figure 2b as TriC 1 and TriC 2 respectively.
The calorimeter sensor and their respective samples were modelled in detail as displayed in Figure 2a. The modelling framework was very similar to the one described in [5], where the model geometry is divided by a $2\,\mathrm{cm} \times 2\,\mathrm{cm} \times 2\,\mathrm{cm}$ spanning over the reactor core.
Irradiations were performed at reactor powers of $100\,\mathrm{kW}$ and $250\,\mathrm{kW}$ respectively. The neutron flux and spectrum were calculated over the above mentioned superimposed mesh using the cell-under-voxel approach [5] in 709 energy groups using the CCFE group structure [12] using the eigenvalue (criticality) calculations. The neutron flux levels were modeled using the normalization described by [13] and following the recorded reactor power in steps. An additional power change step was modelled if the last modelled power differed by more than $0.5\,\%$ from the reactor power log as displayed in Figure 1. Although the JSIR2S has the capability to calculate the isotopic inventory on changing geometry, for instance with different control rod positions at reactor power of $100\,\mathrm{kW}$ and $250\,\mathrm{kW}$, the part of the model with change in the geometry has to be omitted from the isotopic calculations. This functionality is still undergoing development and has not yet been fully tested. It was therefore decided to use the mean control rod position for the calculation of the isotopic inventory and delayed radiation simulations. This approach was also used in previous work with similarly small changes to control rod positions, showing little effect on the delayed gamma field calculations [14]. The changes in k_{eff} and $\bar{\nu}$ between the two configurations were however taken into account. The experiments rely on temperature difference measurements, which take some time to establish. In our case those times range from $42\,\mathrm{min}$ to $55\,\mathrm{min}$. In case of simulations, the heating power can be obtained for a single time. In the present work, the simulated heating level is deduced at the time, corresponding to the temperature measurement during the experiment. However, work is already underway to calculate heating levels at several interval prior to the time corresponding to temperature measurement, and calculate the average (possibly the exponential moving average).

The nuclear heating inside the sample as well as over the entire calorimeter geometry was tallied using TMESH functionality of the MCNP. Compared to the previous JSIR2S version, the MCNP code was modified to make use of TMESH, since it can only be parallelized using MPI [15], requiring and additional function for communicating the custom source routine variables from the head node to its workers. The particle transport in the case of prompt simulations, neutron, photon and electron transport was performed, while photon and electron transport was performed for the delayed simulations. Both were performed using the standard ENDF/B-VIII.0 nuclear data library. This library was also used for the depletion calculations with FISPACT-II-5.00 [12] as part of the JSIR2S package. While the use of ERPDATA [16] is encouraged for electron transport below $1\,\mathrm{keV}$ energies, the electron range at those energies

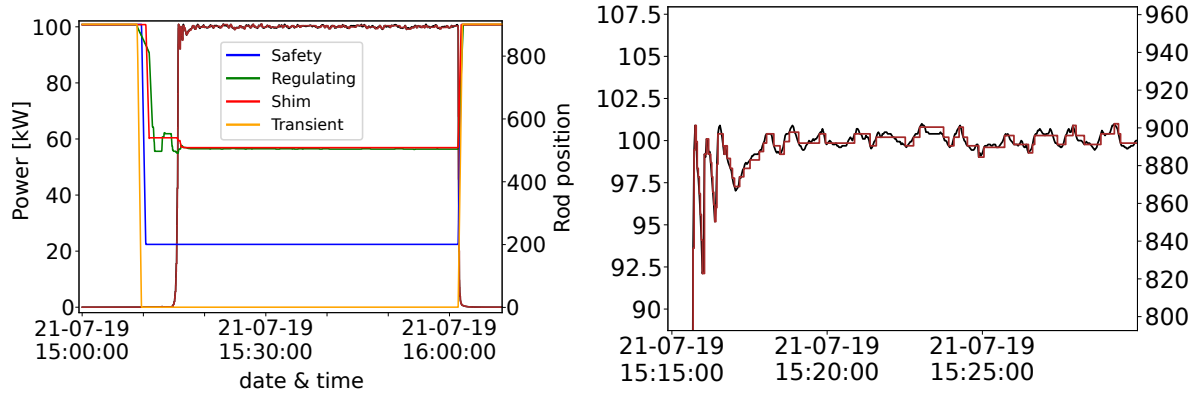

(a) Reactor power and control rod positions.

(b) Close-up of reactor power recording (in black) with modelled power change steps (in brown).

Figure 1: Recorded (black) and modelled (brown) reactor power and control rod positions (position 900: fully inserted) during irradiation of calorimeter without sample at steady reactor power of 100 kW.

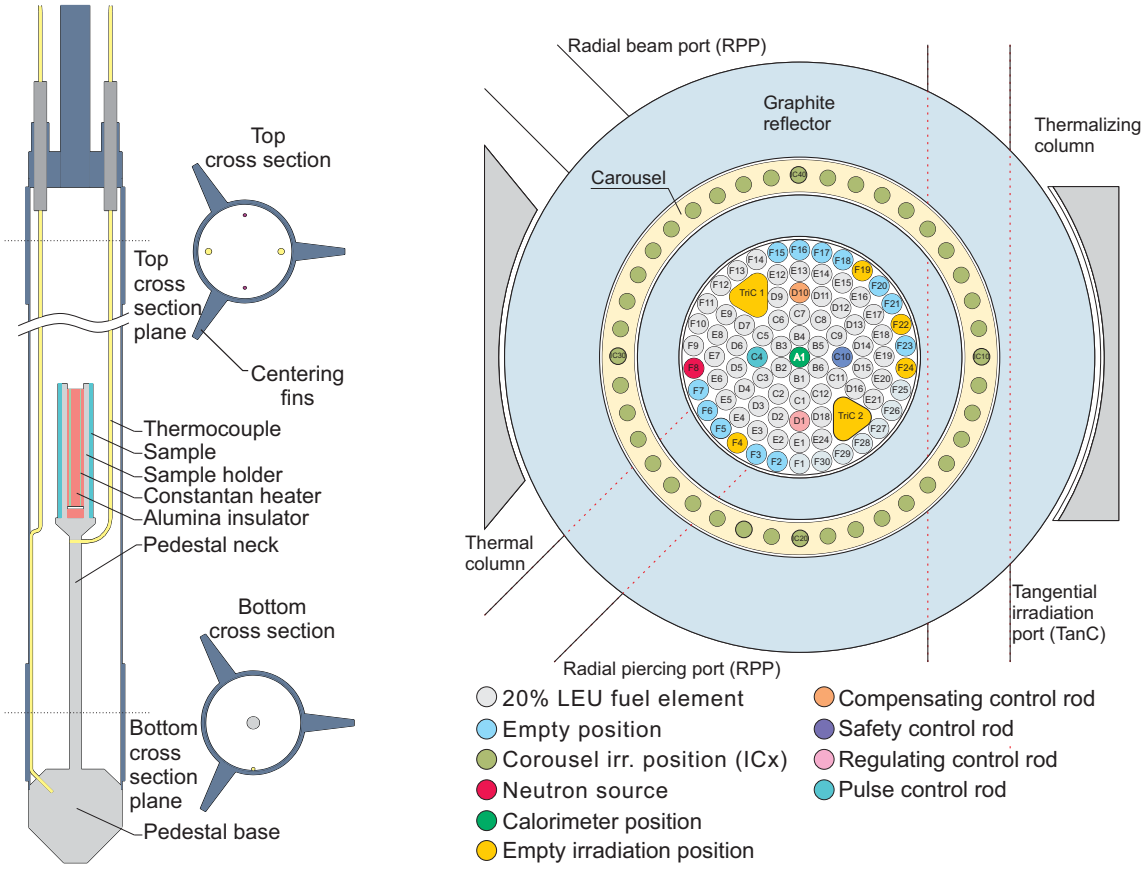

(a) Schematic display of the calorimeter MCNP model.

(b) Configuration of the JSI TRIGA reactor core during experiments.

Figure 2: Calorimeter MCNP model (left) and JSI TRIGA core configuration during the experimental campaign (right).

are of the order of $1 \times 10^{-2}\,\mathrm{mm}$ to $1 \times 10^{-1}\,\mathrm{mm}$ [17], and even lower for the thinnest tungsten sample.
In order to increase the statistics, the Central irradiation channel, it's internals and the calorimeter assemblies has higher importance set for all particle types. The nuclear heating tallies were calculated on a cylindrical mesh superimposed over the pedestal, heater and sample part of the calorimeter, with distinct tallies for total, neutron, photon and electron energy deposition. It should be noted that in case photon tallies, kerma approximation is assumed.
The temperature measurement times and nuclear heating simulation times are given in Table 2.

Table 1: Summary of temperature measurements and simulation times of the nuclear heating experimental campaign

Measurement no.	Sample material	Reactor power [kW]	Measurement date	Measurement time
1	Eurofer 97	100	20.07.2021	12:22:00
2	Eurofer 97	100	20.07.2021	12:29:00
3	Eurofer 97	250	20.07.2021	13:45:00
4	Graphite R6650	100	20.07.2021	15:35:00
5	Graphite R6650	100	20.07.2021	16:08:30
6	Graphite R6650	250	21.07.2021	09:37:00
7	Tungsten 99.95 %	100	21.07.2021	11:04:12
8	Tungsten 99.95 %	100	21.07.2021	11:09:36
9	Tungsten 99.95 %	250	21.07.2021	12:27:00
10	Al 6063	100	21.07.2021	14:16:40
11	Al 6063	250	21.07.2021	14:27:45

3 RESULTS AND COMPARISON WITH MEASUREMENTS

In this section we present the results of the simulations and their comparison with measurements. The simulation results are presented in terms of contributions from prompt and delayed radiation, and further dividing their contributions to individual particle types (neutrons, photons, electrons). An example of prompt and delayed contributions to nuclear heating from all particle types to the graphite sample irradiated at reactor power of $100\,\mathrm{kW}$ is presented in Figure 3. Simulation results are compared with measurements in Table 2 and individual simulation radiation type contributions shown in Table 3. Experimental results for the graphite sample are not shown due to low confidence in the measured results and an identified machining issues with the sample. As mentioned, the rest of the material samples show non-linear temperature responses, which suggests the irradiations were performed at powers outside the linear regime.

We observe, that the calculated heating values are generally substantially lower compared to experiments, in some cases by over $50\,\%$. Although we note, that some approximations are made with respect to simulating the nuclear heating at a single point, the reactor power and thus the induced nuclear heating does not change by more than $5\,\%$. Whether this discrepancy can be attributed to the non-linear effects due to the experiments, nuclear data or something else missing in the simulations, is yet to be investigated with additional experimental data at a lower reactor power.
We can also distinguish between prompt and delayed contributions, contributions of individual particle types and under/over estimation of photon heating using kerma approximation only

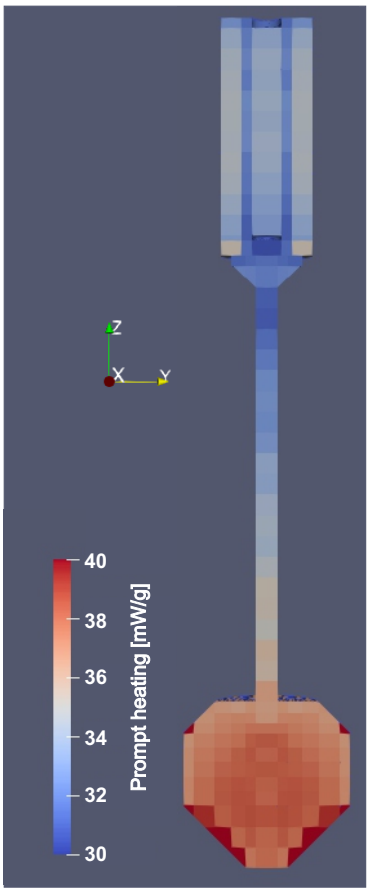

Figure 3: Nuclear heating due to prompt radiation on the pedestal of a calorimeter with graphite sample, during irradiation at $100\,\mathrm{kW}$.

Table 2: Summary of temperature measurements and simulation times of the nuclear heating experimental campaign. Measured values N/A are not available.

Sample material	Measur. numbers	Reactor power [kW]	Simulated heating value [$\mathrm{mW\,g^{-1}}$]	Simulated heating uncertainty [%]	Measured heating [$\mathrm{mW\,g^{-1}}$]	C/E-1 [%]
Eurofer97	1,2	100	46.8	1.7	52.8	−11.4
Eurofer97	3	250	118.7	2.4	129.0	−8.0
Graphite	4,5	100	43.9	1.3	N/A	N/A
Graphite	6	250	109.4	1.9	N/A	N/A
Tungsten	7,8	100	88.5	1.3	112.6	−21.4
Tungsten	9	250	224.7	2.0	275.0	−18.3
Aluminium	10	100	38.5	1.7	53.8	−28.4
Aluminium	11	250	84.7	1.3	131.0	−35.3

(without the transport of charged particles). In case of tungsten samples, with the sample thickness of $0.1\,\mathrm{mm}$ this approximation differs from the real value by almost $25\,\%$.

Table 3: Summary of different contributions to the total nuclear heating. All values in $\mathrm{mW\,g^{-1}}$ of sample material. Photon contribution is given in kerma approximation and as the dose from resulting electrons

Measur. numbers	Prompt				Delayed		
	total	neutron	photon kerma	electron	total	photon kerma	electron
1	36.1	0.9	36.7	35.2	10.5	10.5	10.5
2	36.4	0.9	37.0	35.5	10.6	10.6	10.6
3	91.3	2.2	92.8	89.1	27.4	27.2	27.4
4	34.2	6.6	26.8	27.5	9.5	9.4	9.5
5	34.1	6.6	26.8	27.4	9.9	9.8	9.9
6	84.7	16.3	66.1	68.1	24.7	24.2	24.7
7	66.5	0.2	81.0	66.3	21.8	25.0	21.8
8	66.3	0.2	80.8	66.1	22.3	25.7	22.3
9	166.4	0.5	202.3	165.9	58.4	67.1	58.4
10	28.9	1.5	26.6	27.4	9.7	9.4	9.7
11	70.5	3.5	65.0	67.0	14.2	13.9	14.2

4 DISCUSSION AND FUTURE OUTLOOKS

We can note that the calculated heating values differ from the simulated ones. There are several possible causes for this inconsistency. It is noted that non-linear effects were observed during the experiment, leading to higher orders of correction, which might introduce biases. On the modelling side, several factors can contribute, to some modelling discrepancies to not taking into account several steps prior to the time of the temperature measurement, to nuclear data.

The JSIR2S has been used for calculations of energy deposition in terms of dose, showing good agreement with measurements [5, 18, 14]. The modelling of geometry and material has been extensively checked against the real situation. The second one can be dismayed in the sense, that the reactor power deviates by no more than $5\,\%$ and that using the exponential moving average to replicate the temperature response of the calorimeter would produce a value equal or lower to the one taken at the measurement point. The results obtained using the ENDF/B-VIII.0 nuclear data libraries will also be checked against simulations using other nuclear data libraries, including the low electron energy libraries, to identify any possible shortcomings in this area.

Another experimental campaign has been performed with all of the above mentioned calorimeter samples at a lower reactor power of $30\,\mathrm{kW}$ and is currently being evaluated. This should remove any inconsistencies with respect to the non-linearities of the calorimeter temperature response. In terms of modelling, heating values at times prior to the temperature measurement will be calculated, and averaged using an exponential moving average with time constants mentioned in the experiment [3] to simulate the detector's response.

In the future, we plan to introduce additional fusion relevant materials to the calorimetry measurements, such as beryllium and copper alloy, which is used in the first wall of ITER, and high temperature superconductor (HTS) tape. Although ITER will use Nb_3Sn superconductors, we are still looking for a suitable sample, which we were not able to obtain for the reported experimental campaign.

5 CONCLUSION

We present the comparison between experimental and simulation nuclear heating evaluation for the first nuclear heating experiment using CEA developed calorimeters at the JSI TRIGA reactor. The simulations are performed using the MCNP v6.1 Monte Carlo transport code for prompt radiation field and the JSIR2S code package for simulations of the delayed radiation field. The calculated heating values are systematically lower compared to measurements, where the difference is highest for tungsten. Current efforts are underway to identify and address the inconsistencies. Additional experiments performed at lower reactor power and better detector responses are currently being evaluated. Further experimental campaigns using material samples such as beryllium and HTS tape are planned for the future.

References

[1] Carcreff, H., Salmon, L., Lepeltier, V., Guyot, J.M., and Bouard, E. Last Improvements of the CALMOS Calorimeter Dedicated to Thermal Neutron Flux and Nuclear Heating Measurements inside the OSIRIS reactor. *EPJ Web Conf.*, 170:04002, 2018.

[2] D. Fourmentel, J-F. Villard, A. Lyoussi, C. Reynard-Carette, G. Bignan, J-P. Chauvin, C. Gonnier, P. Guimbal, J-Y. Malo, M. Carette, A. Janulyte, O. Merroun, J. Brun, Y. Zerega, and J. André. Combined analysis of neutron and photon flux measurements for the Jules Horowitz Reactor core mapping. In *2011 2nd International Conference on Advancements in Nuclear Instrumentation, Measurement Methods and their Applications*, pages 1–5, 2011.

[3] Hubert Carcreff, Vladimir Radulović, Damien Fourmentel, Klemen Ambrožič, Christophe Destouches, Luka Snoj, and Nicolas Thiollay. Nuclear heating measurements for fusion and fission relevant materials in the JSI TRIGA reactor. *Fusion Engineering and Design*, 179:113136, 2022.

[4] Ambrožič, Klemen, Fourmentel, Damien, Carcreff, Hubert, Radulović, Vladimir, and Snoj, Luka. Computational support on the development of nuclear heating calorimeter detector design. *EPJ Web Conf.*, 225:04033, 2020.

[5] K. Ambrožič and L. Snoj. JSIR2S code for delayed radiation simulations: Validation against measurements at the JSI TRIGA reactor. *Progress in Nuclear Energy*, 129:103498, 2020.

[6] John T. Goorley, Michael R. James, et al. Initial MCNP6 Release Overview - MCNP6 version 1.0.

[7] D.A. Brown, M.B. Chadwick, et al. ENDF/B-VIII.0: The 8th Major Release of the Nuclear Reaction Data Library with CIELO-project Cross Sections, New Standards and Thermal Scattering Data. *Nuclear Data Sheets*, 148:1–142, 2018. Special Issue on Nuclear Reaction Data.

[8] A. Trkov, G. Žerovnik, L. Snoj, and M. Ravnik. On the self-shielding factors in neutron activation analysis. *Nuclear Instruments and Methods in Physics Research Section A: Accelerators, Spectrometers, Detectors and Associated Equipment*, 610(2):553–565, 2009.

[9] K. Ambrožič, G. Žerovnik, and L. Snoj. Computational analysis of the dose rates at jsi triga reactor irradiation facilities. *Applied Radiation and Isotopes*, 130:140–152, 2017.

[10] Tanja Goričanec, Sebastjan Rupnik, Anže Jazbec, and Luka Snoj. On the optimisation of large sample in-core irradiation channel in the JSI TRIGA reactor. In Luka Snoj and Aljaž Čufar, editors, *NENE 2020: 29th International Conference Nuclear Energy for New Europe*, NENE 2020: 29th International Conference Nuclear Energy for New Europe, page 8. Nuclear Society of Slovenia, 2020.

[11] Anže Jazbec, Sebastjan Rupnik, Vladimir Radulović, Jan Malec, Andraž Verdir, Marko Rosman, Borut Smodiš, and Luka Snoj. Jožef Stefan Institute TRIGA research reactor activities in the period from September 2019 - August 2020. In Luka Snoj and Aljaž Čufar, editors, *NENE 2020: 29th International Conference Nuclear Energy for New Europe*, NENE 2020: 29th International Conference Nuclear Energy for New Europe, page 8. Nuclear Society of Slovenia, 2020. Bibliografija na koncu prispevka.

[12] Greg Bailey, David Foster, Priti Kanth, and Mark Hilbert. The FISPACT-II User Manual. Technical Report UKAEA-CCFE-RE(21)02, UK Atomic Energy Authority, 2021.

[13] Gašper Žerovnik, Manca Podvratnik, and Luka Snoj. On normalization of fluxes and reaction rates in MCNP criticality calculations. *Annals of Nuclear Energy*, 63:126–128, 2014.

[14] G. Kramberger, K. Ambrožič, U. Gürer, B. Hiti, H. Karacali, I. Mandić, E. Yilmaz, O. Yilmaz, and M. Zavrtanik. Development of mos-fet dosimeters for use in high radiation fields. *Nuclear Instruments and Methods in Physics Research Section A: Accelerators, Spectrometers, Detectors and Associated Equipment*, 978:164283, 2020.

[15] Message Passing Interface Forum. *MPI: A Message-Passing Interface Standard Version 4.0*, June 2021.

[16] H. Grady III Hughes. An Electron/Photon/Relaxation Data Library for MCNP6. Technical Report LA–UR–13–27377, Los Alamos National Laboratory, 2013.

[17] M.J. Berger, J.S. Coursey, M.A. Zucker, , and J. Chang. ESTAR, PSTAR, and ASTAR: Computer Programs for Calculating Stopping-Power and Range Tables for Electrons, Protons, and Helium Ions. `http://physics.nist.gov/Star`, 2005.

[18] A. Gruel, K. Ambrožič, C. Destouches, V. Radulović, A. Sardet, and L. Snoj. Gamma-heating and gamma flux measurements in the jsi triga reactor: Results and prospects. *IEEE Transactions on Nuclear Science*, 67(4):559–567, 2020.